Photoionization Spectroscopy of the Zinc Monoethyl Radical and Its Cation

Michael B. Pushkarsky, Vadim L. Stakhursky, and Terry A. Miller*

Laser Spectroscopy Facility, Department of Chemistry, The Ohio State University, 120 W. 18th Avenue, Columbus, Ohio 43210

Received: June 12, 2000; In Final Form: August 4, 2000

The spectra of the ZnC_2H_5 radical and its cation have been recorded by two photoionization techniques, resonantly enhanced multiphoton ionization and zero electron kinetic energy spectroscopy, respectively. The ionization potential of the radical has been determined along with a number of vibrational frequencies in the ground state of the cation and the excited state of the neutral. Based upon the spectroscopic data, models for the metal−carbon bonding in metal alkyl radicals are proposed that predict relative bond strengths for a number of species.

I. Introduction

In recent years there has been considerable interest in the Group IIa and IIb metal methyl radicals M, where M = Mg, Ca, Zn, and Cd. These radicals have been shown to be intermediates in the fabrication of solid-state devices.[1] The cation of $MgCH_3$ is interesting as a prototypical ionic intermediate in Grignard reactions. The rotational and vibronic structure in both the ground and the first electronically excited states of all four radicals have been studied spectroscopically.[2−8] More recently, zero electron kinetic energy (ZEKE) spectroscopy studies have yielded[9,10] adiabatic ionization potentials (AIPs) and vibrational frequencies for the ground state of the cation for the Mg-, Zn-, and Cd-containing species. In a recent publication, a wealth of spectroscopic data for all four species has been summarized.[10] The authors also discussed how the experimentally measured values of electronic excitation and ionization energies can be used to qualitatively estimate the strength of metal−carbon bonds and to predict that the substitution of methyl by a larger alkyl group would weaken the Zn−C bond.

The existing spectroscopic data on larger alkyl group radicals is much sparser than that for methyl-containing ones. To date, the moderate resolution laser-induced fluorescence[11,12] (LIF) spectrum of the $\tilde{X}^2A'-\tilde{A}^2A'$ electronic transition of the ZnC_2H_5 radical and its dispersed fluorescence spectra have been reported. The LIF spectrum of the origin band of a corresponding electronic transition of the CdC_2H_5 radical also has been reported,[11] but no other vibronic structure was observed, most likely due to predissociation.

To address the lack of information on organometallic reactive intermediates with larger alkyl groups, we have performed photoionization spectroscopic studies of ZnC_2H_5 radical and its cation. In this paper, we report the two-color resonantly enhanced multiphoton ionization (REMPI) and ZEKE spectra of the ZnC_2H_5 radical. The goal of the REMPI experiment was severalfold. It was used as a prerequisite to ZEKE experiments to optimize radical production and mass spectrometer performance as well as to ensure that the carrier of the ZEKE spectrum was indeed ZnC_2H_5 by requiring the frequency of the first photon to be in resonance with a known level of the previously identified excitation spectrum of the radical. Another goal was to take advantage of the mass selectivity of the ion detection system to discriminate among spectra belonging to various Zn isotopomers. In addition to the work detailed in this paper, a high-resolution (≈120 MHz) laser system[7] was also used to record both rotationally and mass resolved REMPI spectra of several of the stronger vibronic transitions of ZnC_2H_5. These spectra, although still fairly complex, are dramatically simplified compared to those previously obtained via the LIF technique. The complete analysis of the high-resolution REMPI spectra is in progress, but preliminary results from that analysis are utilized for some of our present assignments.

The present work further demonstrates that ZEKE spectroscopy[13,14] is a powerful tool to investigate the vibrational structure of cations via photionization of corresponding neutral species. Application of this technique to an open-shell radical can produce a closed-shell cation that cannot be prepared via direct ionization of any stable (closed-shell) neutral. Another powerful feature of the two-color REMPI scheme is the possibility to choose different intermediate vibronic levels while recording ZEKE spectra in the same spectral region. The resulting line-to-line intensity variations corresponding to excitation of different intermediate levels have proven to be very useful for securing vibrational assignments for both the cation and the intermediate, electronically excited state of the neutral. Finally, the ZEKE experiment allows for a very accurate determination of an important thermochemical property, the adiabatic ionization potential (AIP) of the corresponding neutral, with an accuracy of a few cm^{-1}.

II. Experiment

The experimental setup has been described elsewhere[9] but a brief summary will be presented here. The ZnC_2H_5 radicals were produced from zinc diethyl (Strem Chemical), by photolysis with an ArF excimer laser lightly focused in front of the nozzle orifice of a supersonic free jet expansion backed by 50−75 psi of He. The pulsed supersonic expansion from a 700 μm nozzle (General Valve), was skimmed by a 2 mm skimmer separating the first chamber from the second, high vacuum, ionization chamber. About 10 cm downstream from the skimmer, the molecular beam passes through the ionization region of the mass spectrometer. For both REMPI and ZEKE pulsed field ionization experiments, the same laser systems were used. The two laser beams have been produced from a pair of dye lasers pumped by the second and third harmonics of a Nd:YAG laser. The

10.1021/jp0021188 CCC: $19.00
Published on Web 09/13/2000

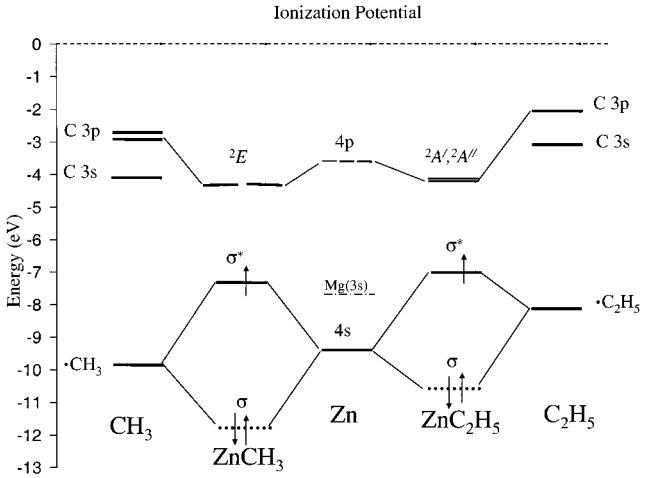

Figure 1. "Experimental" molecular orbital diagrams for $ZnCH_3$ and ZnC_2H_5. For clarity, only orbitals relevant to zinc−carbon bonding are shown. Please note that the lower symmetry of ZnC_2H_5 splits the degeneracy of the LUMO orbital (having E symmetry in $ZnCH_3$) into a pair of closely spaced orbitals. The IP of the Mg atom is shown as well (see text).

output of one of the dye lasers, pumped by the third harmonic of the Nd:YAG, was used to excite the neutral radicals to the electronically excited state (excitation laser). The frequency-doubled output of the second dye laser beam was used to ionize the electronically excited radical (ionization laser).

Optogalvanic spectroscopy using an Fe/Ne hollow cathode lamp was employed to calibrate the fundamental frequency of the ionization laser. The excitation laser was calibrated using previously reported frequencies of the individual vibronic levels of the $\tilde{A}-\tilde{X}$ transitions of the ZnC_2H_5 radical. Despite the fact that the employed calibration procedure gives accuracy of 0.5 cm^{-1}, the reported frequencies of individual bands in the ZEKE spectra are believed to be accurate only to about 3 cm^{-1} due to their relatively broad (10−15 cm^{-1} fwhm) unresolved rotational contour.

Although the general setup is the same for the REMPI and ZEKE experiments, the ionization and detection schemes are different. In the REMPI experiment the excitation laser is scanned through the vibrational levels of the excited electronic state while the ionization laser is kept at a fixed frequency sufficiently energetic to ionize the excited molecules and a time-of-flight mass spectrometer is used to detect ions. In the ZEKE experiment, the excitation laser is kept at a fixed frequency tuned to a transition between the ground electronic state vibrationless level and a particular vibronic level of the intermediate electronic state while the ionization laser is scanned from the ionization energy threshold through the region of interest. In the ZEKE experiment, the lower plate of the ionization region was pulsed 1 μs after the ionization laser was fired to a voltage between −5 and −15 V to pulse-ionize high Rydberg states. The (zero-energy) electrons, emerging after the pulsed-field ionization were detected by the mass spectrometer.

III. Results

Figure 1 illustrates the nature of the electronic transitions in both ZnC_2H_5 and $ZnCH_3$ radicals. The $\tilde{A}^2E-\tilde{X}^2A_1$ electronic transition of the $ZnCH_3$ radical corresponds to promotion of an unpaired electron from an antibonding a_1 symmetry HOMO to a nonbonding doubly degenerate LUMO of e symmetry formed from the $4p_x$ and $4p_y$ orbitals of the zinc atom. In ZnC_2H_5 the substitution of the methyl group by ethyl lowers the molecular symmetry from C_{3v} to C_s and therefore splits the E electronic state into a pair of closely lying states of A′ and A″ symmetry, both optically accessible from the ground electronic state. In a molecular system whose electronic degeneracy is lifted by an asymmetric substitution, significant spin−orbit and vibronic coupling between the resulting pair of electronic states is expected. The spin−orbit interaction leads to large effective spin-rotation effects that complicate the rotational spectra but are insignificant on the scale of the vibronic structure observed in these experiments. On the other hand, the vibronic interactions between the A′ and A″ states can affect both the intensity and frequency of individual vibronic bands and, in particular, may enable nominally forbidden transitions, involving excitation of asymmetric vibrations, to gain intensity in the electronic spectra.

A. Computational Details. In assigning the experimentally observed REMPI and ZEKE spectra, it is extremely useful to have good estimates of vibrational frequencies, electronic excitation energies, etc. A recent study[10] has shown that the density functional theory (DFT) is well suited to the calculation of the geometries, vibrational frequencies, and electronic excitation energies for radicals of this nature. Therefore, we have used B3LYP functional with a 6-311+G(d) basis set to calculate vibrational frequencies for the ground electronic states of both the neutral and cation of ZnC_2H_5 using Gaussian 98 software. The calculated vibrational frequencies of all 18 normal modes are summarized in the Table I. Pooley et al.[12] have previously used the ROHF method to calculate the vibrational frequencies for the $\tilde{X}^2A'$electronic state of ZnC_2H_5. The comparison of the two calculations shows that the ROHF frequencies reproduce the experimental frequencies comparably to the DFT calculations after scaling the former by a factor of 0.89. In addition to vibrational frequencies the adiabatic ionization energy and the energy of the lowest excited A″ state (and its vibrational frequencies) have been calculated. This excited state is believed (see next subsection) to correspond to the $\tilde{B}^2A''$ state. We have not attempted to do similar calculations on the $\tilde{A}^2A'$electronic state because of the complications associated with calculation of a second excited electronic state of a given symmetry. However, we believe that the vibrational frequencies and excitation energies of both the $\tilde{A}$ and $\tilde{B}$ state should be very similar, so our calculations serve as a guide for the $\tilde{A}^2A'$ state as well.

B. REMPI Spectroscopy of the Radical. The moderate resolution REMPI spectrum of the zinc ethyl radical is shown in Figure 2 along with a number of its vibronic assignments. The seven bands in the REMPI spectrum labeled #1−#7 have been used as intermediate transitions to record ZEKE spectra. The REMPI spectrum is very similar to the previously reported LIF spectrum[11,12] (with the exception that it is not obscured by features belonging to zinc hydride that are present in the LIF spectrum but eliminated in the REMPI spectrum due to mass selectivity). The high (120 MHz) resolution rotationally resolved LIF and REMPI spectra of several bands have also been recorded, and although their rotational analysis is still in progress, preliminary results from the analysis are used as guidance (see below) for some vibronic assignments.

The strongest band in the REMPI spectrum at 22 515 cm^{-1} corresponds to the origin of the $\tilde{A}-\tilde{X}$ transition. While the rotational analysis of the high-resolution spectrum of the origin is not complete, it appears that this band is best described as a hybrid a/b type transition. Therefore, the first excited state of zinc ethyl radical must be of $^2A'$ electronic symmetry, since transitions to an A″ state must be c-type. Obviously the $\tilde{B}$ electronic state must have $^2A''$ symmetry.

TABLE 1: Experimental and Calculated Vibrational Frequencies[a] of ZnC_2H_5 Radical and Its Cation

			$\tilde{X}^2A'$		$\tilde{A}^2A'$		$\tilde{X}^{+\,1}A'$	
mode	description[e]	sym	(exp[b])	(calc[d])	(exp[b,f])	(calc[d,g])	(exp[c])	(calc[d])
ν_1	CH_3 stretch	a′		3053		3111		3098
ν_2	CH_2 stretch	a′		3033		3074		3089
ν_3	CH_3 stretch	a′		2925		2994		2976
ν_4	CH_3 bend	a′		1512		1515		1505
ν_5	CH_2 bend	a′		1467		1480		1468
ν_6	CH_3 bend	a′		1420		1413	1380	1403
ν_7	CH_2/CH_3 wag (ip)	a′	1101	1120	1087[c]	1131	1107	1152
ν_8	C−C stretch	a′	987	1001	1011	1021	1015	1035
ν_9	CH_2/CH_3 wag (ap)	a′	915	924		947	933	920
ν_{10}	Zn−C stretch	a′	387	353	424	432	424	387
ν_{11}	Zn−C−C bend	a′	180	179	245	222	217	218
ν_{12}	CH_3 stretch	a″		3096		3192		3171
ν_{13}	CH_2 stretch	a″		3073		3113		3146
ν_{14}	CH_3 bend	a″		1516		1518		1462
ν_{15}	CH_2/CH_3 twist (ap)	a″		1245		1243		1238
ν_{16}	CH_2/CH_3 twist (ip)	a″		896		937		920
ν_{17}	CH_2 rock	a″		578		735	683	697
ν_{18}	CH_3 torsion	a″		202	218[h]	253	238	248

[a] All values in cm^{-1}. [b] From Pooley et al.,[12] unless otherwise indicated. [c] This work. [d] Density functional theory calculations, see text for details. [e] Mode description is approximate and adopted from ref 12; ip = in phase; ap = antiphase. [f] The experimental frequency of the origin of the $\tilde{X}^2A'-\tilde{A}^2A'$ transition is $T_{00} = 22515$. [g] The listed frequencies are actually calculated for the lowest excited A″ state, but the frequencies are expected to be rather similar for the close-lying $\tilde{A}^2A'$ and $\tilde{B}^2A''$ states. [h] Frequency deduced from overtone band.

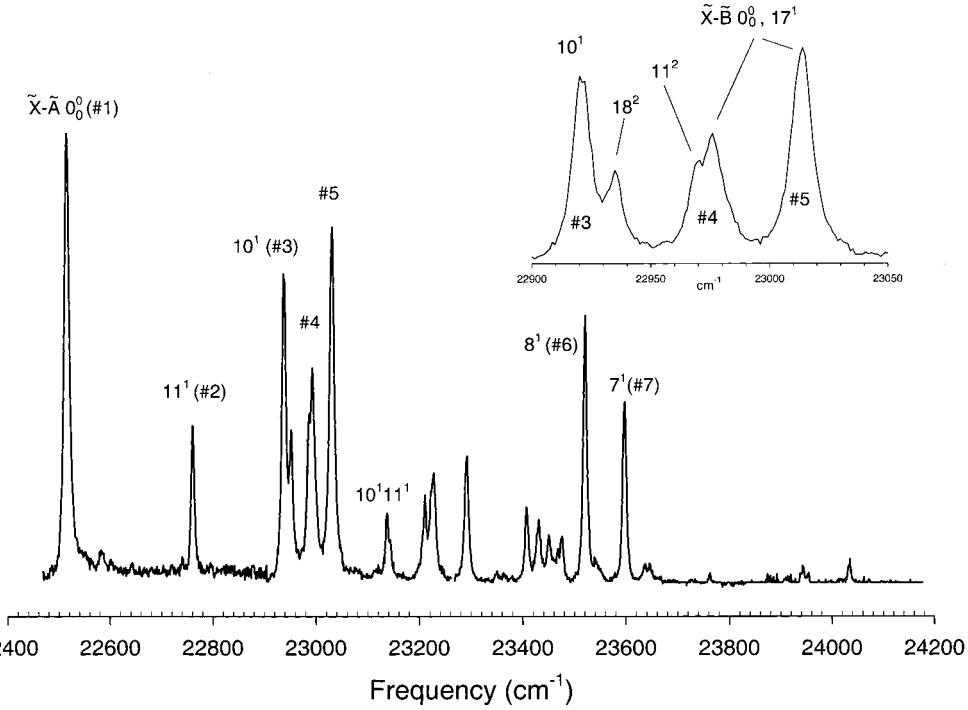

Figure 2. REMPI spectrum of the ZnC_2H_5 radical. Vibronic assignments are indicated above a number of transitions. The labels #1−#7 indicate seven vibronic levels used as intermediate states to record two-photon ZEKE spectra. The insert shows in greater detail the structure and assignment of a congested region between band #3 and #5. For two transitions (upper frequency component of #4 and #5) two alternative vibronic assignments are given (see text for more details).

Our assignments of the REMPI spectrum are based on the previously reported spectral work and the results of the ab initio calculations given in Table 1. A few prominent features in the spectrum have been tentatively assigned previously,[12] using ab initio frequency calculations and the analysis of the intensity variations in the dispersed fluorescence spectra. The band (labeled #2 in Figure 2) at 22 760 cm^{-1} has been assigned as the fundamental of the in-plane Zn−C−C bend, 11^1. The strong feature (#3) at 22 939 cm^{-1} has been assigned as the Zn−C stretch, 10^1 while the nearby weaker feature (not labeled) at 22 951 cm^{-1} is most probably 18^2, the overtone of the lowest asymmetric vibration—the methyl torsion. The relatively broad feature (#4) at 22 990 cm^{-1} (490 cm^{-1} above the origin) consists of two partially overlapping vibronic transitions. The lower frequency one is definitely the overtone of the Zn−C−C bend, 11^2, while the upper frequency one has not been assigned previously. However, the preliminary rotational analysis of the high-resolution REMPI spectra of this band suggests a c-type transition consistent with its upper state having A″ vibronic symmetry. It appears that the only reasonable assignments of this band are as either the vibrationless level of the $\tilde{B}^2A''$ electronic state or the fundamental of ν_{17}—an a″ CH_2 rocking mode in the $\tilde{A}^2A'$ electronic state (predicted to have a frequency of 578 cm^{-1} for radical). No other unaccounted vibronic levels,

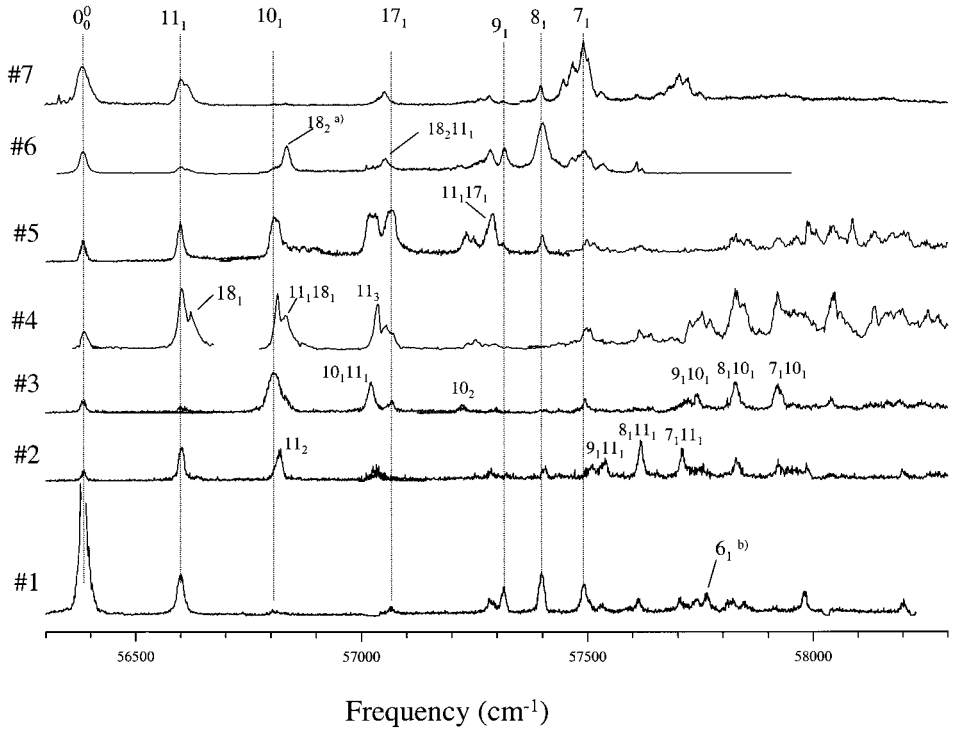

Figure 3. ZEKE spectrum of the ZnC_2H_5 radical. The labels #1−#7 indicate respectively the seven vibronic levels (assigned in the text and labeled on Figure 2) used as intermediate states to record the two-photon ZEKE spectra. The vibrational assignment is given for most of the observed transitions. Note the intensity variations between different traces, most notably for the bands 10_1 and 17_1. The bands 18_2 and $18_2\,11_1$ in trace #6 may be alternatively assigned as $18_1\,11_1$ and $18_1\,11_2$ respectively (see the text). The band tentatively assigned as ν_6 in trace #1 may be alternatively assigned as a different C−H bend, ν_5 (see Table 1).

symmetric or asymmetric, are expected in this frequency region. The nearby strong band labeled #5 residing at 532 cm^{-1} above the origin of the $\tilde{A}^2A'$ state has been previously tentatively assigned by Pooley et al.[12] as the vibrationless level of the $\tilde{B}^2A''-\tilde{X}^2A'$ electronic transition based upon strong emission at the pump frequency in the dispersed fluorescence spectrum. If we accept this assignment for band #5 then the upper frequency component of the band #4 must be 17^1. However, these two assignments could be switched and, at present, the available experimental data (including ZEKE spectra) do not provide sufficient evidence to rule out either assignment. However, what is perhaps even more important, these two bands are separated only by 42 cm^{-1} and are most likely strongly mixed by vibronic interactions and, hence, unique assignments are not strictly meaningful.

The strong band (#6) at 23 526 cm^{-1} has been previously assigned as a symmetric C−C stretch, 8^1. Finally, we have assigned the previously unassigned band (#7) at 23 602 cm^{-1} as a symmetric CH_2/CH_3 wag, 7^1, based upon ab initio calculations and the intensity pattern in the ZEKE spectra of the cation, as will be discussed below. No strong transitions have been observed at frequencies above 23 600 cm^{-1}, likely due to poor Franck−Condon factors and/or the opening of a nonradiative process, similar to that observed in $CdCH_3$ radical.[15] The vibrational information for the ZnC_2H_5 radical is summarized in the Table I.

C. ZEKE Spectrum of the $\tilde{X}^+\,{}^1A'$ Electronic State of the ZnC_2H_5 Cation. The two-photon resonant ZEKE spectrum of the $\tilde{X}^+\,{}^1A'$ ground electronic state of the zinc monoethyl cation has been recorded in the range of 56 400−58 500 cm^{-1} above the origin of the ground electronic state of the neutral. In the course of our experiments seven ZEKE traces (in the same total energy range) were recorded by tuning the first (excitation) laser successively to the seven different vibronic transitions of the intermediate electronic state of the radical, labeled #1 through #7 in the REMPI spectrum of Figure 2. The recorded traces feature alternations in the relative intensities of the individual vibrational transitions due to variations in the vibronic character of the intermediate state. Analysis of such alternations is very important for securing reliable vibrational assignments of the ZEKE spectra.

All seven traces of ZEKE spectrum are shown in Figure 3. The lowest frequency feature in the ZEKE spectrum at 56 384 cm^{-1}, present (with various intensities) in all traces is, clearly, the vibrationless level of the $\tilde{X}^+\,{}^1A'$ state of ion. Accessible voltage variations in the ionization region showed no clearly discernible shift of this line. Therefore, we take 56 384(5) cm^{-1} as the value of the adiabatic ionization potential (AIP) of ZnC_2H_5 radical, where the error reflects both the line's breadth and possible residual undetected field shifts. The totality of the spectra presented in Figure 3 reveals extensive vibrational structure for an energetically isolated $\tilde{X}^+\,{}^1A'$ ground electronic state of zinc ethyl cation.

Below we discuss the analysis of all seven traces of ZEKE spectra. The resulting experimental frequencies of six symmetric and two asymmetric vibrations are given in the Table 1, along with their values from the ab initio calculation.

1. ZEKE Spectra via Bands #1, #2, and #3. The trace labeled #1 in Figure 3 of the ZEKE spectrum, taken via the origin of the $\tilde{A}^2A'$ excited electronic state of the radical features a very strong origin band for the cation at 56 384 cm^{-1} and a somewhat weaker transition at 56 604 cm^{-1} (217 cm^{-1} above origin), which obviously is the fundamental of the Zn−C−C in-plane bend, 11_1. A very weak overtone 11_2 at 56 816 cm^{-1} is also observed. Three relatively strong transitions at 57 318, 57 400, and 57 492 cm^{-1} have been assigned respectively as fundamentals of the symmetric vibrational modes, ν_9 (CH_2/CH_3 antiphase wag), ν_8 (C−C stretch), and ν_7 (CH_2/CH_3 in-phase

wag) based upon their close match with ab initio calculated frequencies and the relatively strong intensities expected for allowed symmetric modes. Trace #2 (via the 11^1 vibrational level in the intermediate electronic state) shows a strong 11_n progression, up to $n = 3$. The features at higher frequency form a pattern very similar to that of the trace #1, but shifted to the blue by about 220 cm^{-1}. Therefore we assign them as combination bands of the previously assigned vibrations 9_1, 8_1, and 7_1 with one quanta of ν_{11}. Trace #3 (via 10^1, the fundamental of the Zn−C stretch) yields a weaker origin, a barely observable 11_1 band and a strong transition at 56807 cm^{-1}, obviously corresponding to the excitation of the Zn−C stretch, 10_1 in the ion. A strong combination band with ν_{11} and a weak overtone 10_2 have been observed as well. Note that the 10_1 transition lies only 8 cm^{-1} to the red of 11_2 (appearing as a small unresolved shoulder on the higher frequency side of the 10_1 band in trace #3), and it is only the intensity pattern variation between traces #2 and #3, that permits its unambiguous assignment. The three stronger transitions at higher frequency are assigned as the combinations 9_110_1, 8_110_1, and 7_110_1.

Finally, one relatively weak band (marked on trace #1) has been clearly observed in the frequency range of 1200−1700 cm^{-1} above the origin (where the C−H bending transitions are expected) and tentatively assigned as the fundamental of the (lowest frequency) symmetric C−H bending vibrational mode, ν_6, although assignment to another C−H bend, ν_5, cannot be ruled out.

2. ZEKE via Bands #4 and #5. The REMPI transitions #4 (upper frequency component) and #5 terminate at the two (vibronically mixed) levels of a″ vibronic symmetry, tentatively assigned as the origin of the electronic state and a fundamental of asymmetric CH_2 rock, ν_{17}, of the $\tilde{A}^2A'$ electronic state. The a″ vibronic character of these intermediate states must be manifested in corresponding ZEKE spectra via (otherwise prohibited) transitions to a″ symmetry vibrational levels in the cationic state. Therefore, one would expect additional transitions corresponding to fundamentals of asymmetric vibrations in ZEKE traces #4 and #5. As seen in Figure 3, the ZEKE spectrum via band #4 is similar to that via band #2; i.e., it features a strong 11_n progression,obviously due to the fact that the lower frequency component of the band #4 corresponds to 11^2 level. However, for each member of the 11_n progression (except the vibrationless level) there is a "satellite" feature on its higher frequency side. The only feasible assignment for the "satellite" of the 11_1 band (located 238 cm^{-1} above origin) is a fundamental of an asymmetric methyl torsion mode, 18_1 (ab initio frequency of 248 cm^{-1}). Obviously higher frequency "satellites" belong to combination bands 11_n18_1, $n = 1,2$. The higher frequency end of the spectrum features rich, but unresolved vibrational structure caused by excitation of both symmetric and asymmetric vibrations. The ZEKE spectrum via band #5 features a prominent transition at 57 067 cm^{-1} (683 cm^{-1} above the origin) as well as strong progressions 11_n and 10_111_m ($n = 0-3$, $m = 0, 1$). Examination of the set of ab initio frequencies clearly shows that the band at 683 cm^{-1} above the origin cannot belong to any symmetric vibration or overtone of an asymmetric vibration, as all low-frequency modes are already accounted for. Therefore, the only likely assignment of this band is 17_1, an asymmetric CH_2 rocking motion, predicted to have a frequency of 697 cm^{-1}. We believe that reliance upon the ab initio predictions is appropriate because (i) all other experimental vibrational frequencies are in reasonably good agreement with predictions, (ii) the next three symmetric modes (ν_9, ν_8, ν_7) are already tentatively assigned in the ZEKE spectrum, and (iii) as mentioned above, the asymmetric vibronic character of the intermediate level is expected to make a transition to an asymmetric vibrational levels in the cationic state possible. Therefore, we assign this band to 17_1. The 17_1 band is also observable in ZEKE traces #1 and #3 (taken via symmetric intermediate levels) though with much weaker relative intensities and probably in trace #4, although in a congested part of the spectrum.

3. ZEKE via Bands #6 and #7. Finally, we discuss the use of the two strong transitions, labeled #6 and #7 in the higher frequency part of the REMPI spectrum, for recording ZEKE spectra. Band #6 was previously assigned (Table 1) as an excitation of one quantum of the C−C stretch, 8^1, in the $\tilde{A}^2A'$ electronic state of the neutral. The ZEKE spectrum via band #6, features a relatively strong origin band, while its strongest feature at 57 400 cm^{-1} corresponds to what we have already assigned in the ZEKE spectrum as the excitation of one quantum, 8_1, of C−C stretch in the ionic state. Clearly, the observed intensity pattern significantly reinforces the assignment for ν_8 in both the excited state of the radical and its cation. Similarly, the ZEKE spectrum via band #7 shows the strongest transition at 57 492 cm^{-1}, which has been previously assigned as 7_1.

There are two bands in traces #6 and #7 of the ZEKE spectrum which need special attention. The first one is observed in trace #6 at a frequency of 56 830 cm^{-1}. While its frequency matches well with that of the 11_118_1 band, observed in trace #4, it is highly improbable that this transition would have strong intensity in trace #6, while the fundamental 18_1 does not. Therefore, we prefer to assign this transition to 18_2, an overtone of the asymmetric torsional mode, which is obviously symmetric and therefore allowed. Then the weaker band residing about 217 cm^{-1} to the blue is readily assigned to 11_118_2. Similarly, a transition observed in trace #7 at 57 052 cm^{-1} eludes unambiguous assignment due to the fact that it is not a part of any progression. The two alternative assignments, made exclusively upon the frequency match, are either 11_218_1 or 11_118_2.

Comparison of the experimentally observed and calculated vibrational frequencies in the cation (Table 1) suggests that of the symmetric bands only two of the C−H bends and the three C−H stretches (with frequencies in the range of 1500 and 3000 cm^{-1}, respectively) have not been identified in the spectrum. Due to the nature of the molecular orbitals involved, the C−H bond distances are not expected to change much upon electronic excitation (or ionization) of the ZnC_2H_5 radical. Consequently, the normal modes involving C−H stretches are expected to have very diagonal Franck−Condon factors (similar to those in the methyl compounds) and we have not attempted to observe them. To the contrary, both REMPI and ZEKE spectra of all the methyl compounds feature relatively strong transitions corresponding to the excitation of the fundamental of ν_2, the symmetric umbrella vibration of the methyl group. Obviously this is a manifestation of a change in the equilibrium HCH angle in the methyl group upon electronic excitation/ionization, confirmed by both the rotational analysis and ab initio calculations.[10] Due to the similarity between methyl- and ethyl-containing species we expect that in the ZnC_2H_5 radical the methylene group equilibrium bond angles must change upon electronic excitation/ionization too. However, one may speculate that, unlike the case of the monomethyl compounds, the bond angles that would "relax" most (upon electronic excitation/ionization) are those which correspond to the less energetic Zn−C−C bending and CH_2/CH_3 wagging motions, rather then higher energy H−C−H bending motion. Therefore, one would not

necessarily expect to see strong transitions corresponding to H−C−H bends in the ZnC_2H_5 radical and its cation, but would expect to observe strong wagging and Zn−C−C bending motions. In accordance with this argument both wagging modes (ν_9 and ν_7) have been observed in the ZEKE spectra of the cation with relatively strong intensities, but only one of the three high-frequency C− H bends was observed and with relative weak intensity.

IV. Discussion

The present ZEKE spectroscopy in conjunction with other spectroscopic information provides a direct probe of the elctronic and vibrational structure of metal−alkyl radicals and cations. Barckholtz et al.[10] have produced a nearly complete set of both neutral and ion equilibrium geometries, vibrational frequencies, electronic excitation energies, and adiabatic ionization potentials for the four methyl compounds, MCH_3 (M = Mg, Ca, Zn, Cd). Similar data presented in this report for the ZnC_2H_5 radical allows one to compare the effect of the size of the alkyl group on the carbon-metal bonding for the Zn alkyl species.

It is useful to follow the "experimental molecular orbital diagram" approach outlined by Barckholtz et al.[10] Figure 1 represents the molecular orbital diagrams for the three molecular fragments: Zn atom, methyl radical, and ethyl radical as well as for the two organometallic radicals of interest: ZnC_2H_3 and ZnC_2H_5. Wherever possible, the energies of molecular orbitals were taken from experimental data: i.e., the experimentally determined ionization thresholds and origins of electronic transitions. The energy of the 4s orbital of the Zn atom[16] was taken to be the negative of the ionization energy of Zn atom. The energy of the electronic 4s−4p transition in Zn was used to place its 4p level on the diagram. Similarly, the energies of valence (unpaired) and several Rydberg MOs for the alkyl radicals were determined from their previously reported[17,18] ionization potentials. The experimental values for the AIPs (obtained from ZEKE spectra) and origins of the $\tilde{X}-\tilde{A}$ electronic transitions of the Zn−alkyl radicals were used to place the HOMO (σ^*) and LUMO (being, in the first approximation, the zinc atomic $4p_{x,y}$ orbitals) for both radicals. Note that the lower (C_s) symmetry of the ZnC_2H_5 radical lifts the degeneracy of the e symmetry LUMO orbital of the $ZnCH_3$, with strong spectroscopic evidence for this splitting being of the order of 600 cm^{-1} (see section II). One can see that while the symmetry lowering causes a dramatic change in the vibronically and rovibronically resolved electronic spectra, its effect on the energy scale relevant to chemical bonding is negligible. The atomic core and C−H σ orbitals are not included in the diagram, as they are not expected to materially participate in Zn−C bonding. The MO diagram constructed for $ZnCH_3$ and ZnC_2H_5 (but qualitatively correct also for Mg-, Ca-, and Cd-containing species) shows that the two orbitals (σ and σ^*) populated in the ground state configuration are formed almost exclusively from the 4s orbital on zinc and the singly occupied HOMO orbital of alkyl group.

The stabilization energy of the σ orbital must be a function of the energy difference between the contributing orbitals of the fragments. As the figure shows, in the case of zinc methyl a very small energy gap leads to a strong interaction and formation of a strong covalent Zn−C bond. Since the ethyl radical has a smaller ionization potential, its valence orbital is located approximately 1.4 eV above the 4 s orbital of the zinc atom in the MO diagram. Therefore, the mixing between the fragment MOs should be smaller and, as a result, the Zn−ethyl bond correspondingly weaker.

The precise measurements of the AIPs for both zinc−alkyl radicals show that this is the case. The MO diagram (Figure 1) shows that the two-photon ionization process employed in the ZEKE experiments removes an unpaired electron from a singly occupied σ^* HOMO radical orbital. Therefore, the values of AIPs for both fragments and the radical allow one to determine the energy of the radical antibonding HOMO relative to the average of the contributing MOs of the Zn atom and the alkyl group. For the zinc monomethyl radical this value is approximately 2.3 eV, while for zinc ethyl it decreases to 1.9 eV. In the approximation that only the two fragment orbitals are involved in the radical MOs, the strength of the bonding interaction of the σ orbital is equal and opposite to that of the antibonding σ^* orbital. Consequently the Zn−C bonding in the $ZnCH_3$ radical is stronger than that in the ZnC_2H_5 radical. Obviously the same is true for the corresponding cation. We also note that in the ground electronic state of the ZnC_2H_5 radical the odd electron is localized on the ethyl group, while the two bonding electrons are localized on zinc. One can see that the increase of energy of the HOMO of ZnC_2H_5 compared to that of $ZnCH_3$ is not due to stronger (anti)bonding interaction between zinc and alkyl group, but rather from the fact that the HOMO orbital of the ethyl fragment has a higher energy than that of the methyl. From this analysis one may predict that substitution of ethyl by a larger alkyl group would lead to even weaker bonding as the AIP in the alkyl radicals decreases with the size: 9.84 eV (CH_3), 8.14 eV (C_2H_5), 7.36 eV (i-C_3H_7), and 6.70 eV (n-C_4H_9).[18]

On the other hand, the relative strengths of bonding in other metal alkyl radicals may be quite different. Consider for example Mg alkyl radicals. Reference to Figure 1 shows that the IP of Mg is much less than that of Zn, and indeed rather close to that of the ethyl radical. Therefore, based upon the above arguments, one would expect the Mg−C bond in MgC_2H_5 to be stronger than the one in $MgCH_3$, just opposite to the case of the Zn alkyl radicals. Clearly, a direct experimental test of this prediction for the Mg alkyl radicals would be most interesting.

V. Conclusions

The vibrationally resolved REMPI and ZEKE spectra of the radical and cation have been reported. A value for the AIP of 56 384 cm^{-1} has been obtained for ZnC_2H_5. The vibrational analysis of the ZEKE spectra has yielded harmonic frequencies for six symmetric and two asymmetric normal modes in the ground electronic state of the cation. The experimental values of the AIPs and the intermediate electronic excitation energies allow the construction of molecular orbital diagrams for ZnC_2H_5 radical like those previously published for $ZnCH_3$. These diagrams as well as the experimental vibrational frequencies provided insight into the nature of metal−carbon bonding in the metal alkyl family of radicals.

Acknowledgment. The authors gratefully acknowledge support of this work by the National Science Foundation via grant CHE-9974404. The authors also thank Brian Applegate for assistance in the ab initio calculations and acknowledge a grant of computer time from the Ohio Supercomputer Center.

References and Notes

(1) Rytz-Froydevaux, Y.; Salathe, R. P.; Gilgen, H. H.; Weber, H. P. *Appl. Phys. A* **1982**, *27*, 133.

(2) Penner, A.; Amirav, A.; Bersohn, R. *Chem. Phys. Lett.* **1991**, *176*, 147.

(3) Brazier, C. R.; Bernath, P. F. *J. Chem. Phys.* **1989**, *91*, 4548.

(4) Marr, A. J.; Grieman, F.; Steimle, T. C. *J. Chem. Phys.* **1996**, *105*, 3930.
(5) Cerny, T. M.; Tan, X. Q.; Williamson, J. M.; Robles, E. S. J.; Ellis, A. M.; Miller, T. A. *J. Chem. Phys.* **1993**, *99*, 9376.
(6) Tan, X.-Q.; Cerny, T. M.; Williamson, J. M.; Miller, T. A. *J. Chem. Phys.* **1994**, *101*, 6396.
(7) Rubino, R.; Williamson, J. M.; Miller, T. A. *J. Chem. Phys.* **1995**, *103*, 5964.
(8) Salzberg, A. P.; Applegate, B. E.; Miller, T. A. *J. Mol. Spectrosc.* **1999**, *193*, 434.
(9) Panov, S. I.; Powers, D. E.; Miller, T. A. *J. Chem. Phys.* **1998**, *108*, 1335.
(10) Barckholtz, T. A.; Powers, D. E.; Miller, T. A.; Bursten, B. E. *J. Am. Chem. Soc.* **1999**, *121*, 2576.
(11) Povey, I. M.; Bezant, A. J.; Corlett, G. K.; Ellis, A. M. *J. Phys. Chem.* **1994**, *98*, 10427.
(12) Pooley, S. J.; Ellis, A. M. *J. Mol. Spectrosc.* **1997**, *184*, 48.
(13) Muller-Dethlefs, K.; Schlag, E. W. *Annu. Rev. Phys. Chem.* **1991**, *42*, 109.
(14) Armentrout, P. B.; Baer, T. J. *J. Phys. Chem.* **1996**, *100*, 12866.
(15) Pushkarsky, M.; Barckholtz, T.; Miller, T. A. *J. Chem. Phys.* **1999**, *110*, 2016.
(16) Moore, C. *Atomic Energy Levels*; NBS: Washington, DC, 1949.
(17) Lengsfield, B. H.; Siegbahn, P. E. M.; Liu, B. *J. Chem. Phys.* **1984**, *81*, 710.
(18) Georgiadis, R.; Armentrout, P. B. *J. Am. Chem. Soc.* **1986**, *108*, 2119.